28TH INTERNATIONAL SYMPOSIUM ON BALLISTICS
ATLANTA, GA, SEPTEMBER 22–26, 2014

STATISTICAL METHOD FOR DETERMINING GOVERNING PROPERTIES OF HIGH-VELOCITY POLYMER PENETRATIONS

Carey D. Price and Todd S. Rushing
US Army Engineer Research and Development Center, 3909 Halls Ferry Road, Vicksburg, MS 39180

Abstract

Determination of the ballistic limit of candidate armor materials is often a purely experimental process involving little more than trial and error. Attempts to predict the ballistic response of novel materials such as polymers are often based on assumed material properties that are poorly understood or have little influence on the overall performance of the material. One such material property that is often overlooked is tan δ, the ratio of a polymer's loss modulus to storage modulus. These values are both rate and temperature dependent and were proposed to dominate the failure of certain ballistic regimes by Roland et al.[1] The focus of this study was to determine what, if any, correlation exists between tan δ and ballistic limit in the specific case of low-mass (2gn), high-velocity (~1800 m/s) projectiles impacting a range of polymers. In the absence of a direct correlation between tan δ and ballistic limit, the study shifted focus to the material properties that dominate failure in these events. Target samples of various commercially available plastics were subjected to laboratory ballistics testing, and the ballistic limit (V_{50}) was determined for each material. The results of the ballistics tests were then compared to the tan δ, loss modulus, and storage modulus of each material as well as other material properties to determine the correlations present and quantify the contribution of each on high-speed, low-mass projectile penetration into polymers.

1. Introduction

Polymers have long been utilized by the defense industry as components in ballistic protection materials. However, due to the relatively low strength and hardness as compared to metallic or ceramic based armors, the use of polymers has generally been limited to composite materials (both fiber and matrix constituents) or as appliqués to stronger, harder materials.[1][2] Homogenous polymer materials may have little or no practical use in the ballistic protection industry, yet an understanding of the physics and dominant failure mechanisms present in these materials may lend them to future development of armor composites or appliqués.

Since polymeric materials behave very differently from traditional armor materials, it can be assumed that the failure mechanisms within the traditional ballistic regime are quite different. Thus, an adequate understanding of polymer behavior at high rates is desirable. Dynamic Mechanical Analysis (DMA) is a standardized method of determining viscoelastic properties of plastic materials over a range of temperatures and frequencies.[3] Materials may be tested in cyclic tension, compression, torsion, or bending depending on the material properties, the capabilities of the DMA instrument, and the needs of the researcher. A typical DMA analysis of a sample includes several frequencies (typically 1, 10 and 100Hz) over a set temperature range (typically 0-150 °C). During the analysis, a cyclic strain is applied to the sample in a sinusoidal fashion, and the driving stress required to achieve the input strain is measured.

Viscoelastic materials exhibit a phase shift between applied stress and resulting strain. This phase angle, δ, has been shown be a function of the storage modulus, E', and the loss modulus, E''. The three properties are related as shown in Equation 1.[4]

$$\frac{E''}{E'} = \frac{sin(\delta)}{cos(\delta)} = tan(\delta) \quad (1)$$

Once ballistic, DMA, and other material properties were compiled for all of the samples, a rudimentary statistical analysis was performed in Minitab. Best-Subsets analyses were conducted for various combinations of material properties as predictors for V_{50}. Properties that were shown to have little or no correlation were not considered, and only a first-order regression was performed.

2. Materials and Methods

Eleven commercial thermoplastics were selected for the present study, and a summary of the material characteristics and sources is provided in Table 1.

Table 1. Polymer Samples.

Identifier	Producer/Supplier	Product Name	Polymer Type	Key Characteristics
1	King Performance Commodities	HDPE	high density polyethylene	inexpensive, good for massive articles
2	Bayer	Makrolon WG	polycarbonate	amorphous, transparent
3	DuPont	Delrin 150	acetal	crystalline, homopolymer
4	Quadrant	TIVAR H.O.T.	UHMW polyethylene	heat stabilized, anti-oxidant filled
5	Quadrant	TIVAR 1000	UHMW polyethylene	ultra-high molecular weight, virgin
6	DuPont	Zytel 42A	Nylon 6/6	natural, extruded nylon
7	DuPont	Zytel 159	Nylon 6/12	low moisture absorption
8	Reynolds	R-cast	acrylic	transparent, commercial acrylic, proprietary formulation
9	King Performance Commodities	ABS	acrylonitrile butadiene styrene	black, easy to machine
10	Ensinger	TECAPET	polyethylene terephthalate	proprietary PET formulation, wear resistant
11	Advanced Polymer Technologies	Semilon PK	poly (ether ether ketone)	highest performance, highest cost

The polymer samples were ordered in 1in. thick panels, and with the exception of PEEK (6 in square), were all 12 in. square.

DMA measurements were performed with a TA Instruments Q800 using the bending method as described in ASTM D4065.[3] The single cantilever configuration was used as shown in Figure **1**. Specimens were machined from stock shapes to final dimensions 35 mm by 12.5 mm by 2.5 mm, and the test span after

clamping into the fixture was 17 mm. The test chamber was cooled to the starting temperature by liquid nitrogen, and the soak time was 2 min after equilibrium was reached. The heating rate was 3 °C/min. The terminal temperature varied depending on the thermal properties of the subject material. The applied strain (displacement) was fixed at 20 microns, and the stepwise loading frequencies were 1, 10, and in some cases 100 Hz.

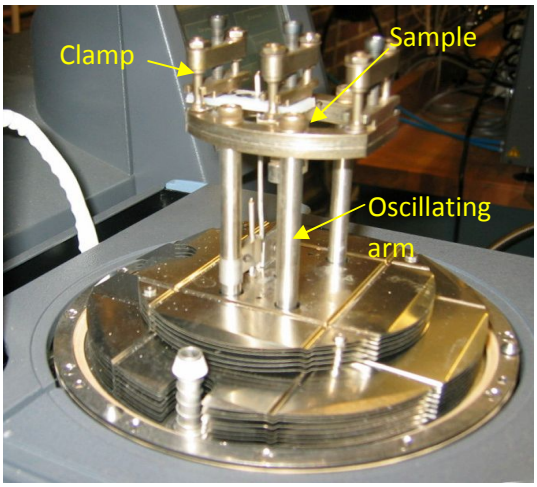

Figure 1. DMA Instrument.

Ballistic testing was conducted at the Engineer Research and Development Center's Ballistic Research Facility using a fixed universal receiver chambered in 0.50 caliber BMG. Testing procedures followed the process detailed by Jordan and Naito.[5] Projectile velocity measurements were typically made using a pair of Oehler Research, Inc. Model 35P proof chronographs, each connected to two Oehler Model 55 light screens as shown in Figure 2; however, due to the small size and relatively high velocity of the projectiles used in this study, these light screens were unable to reliably detect the projectiles. Thus, an independent high-speed video camera was required to measure impact velocity.

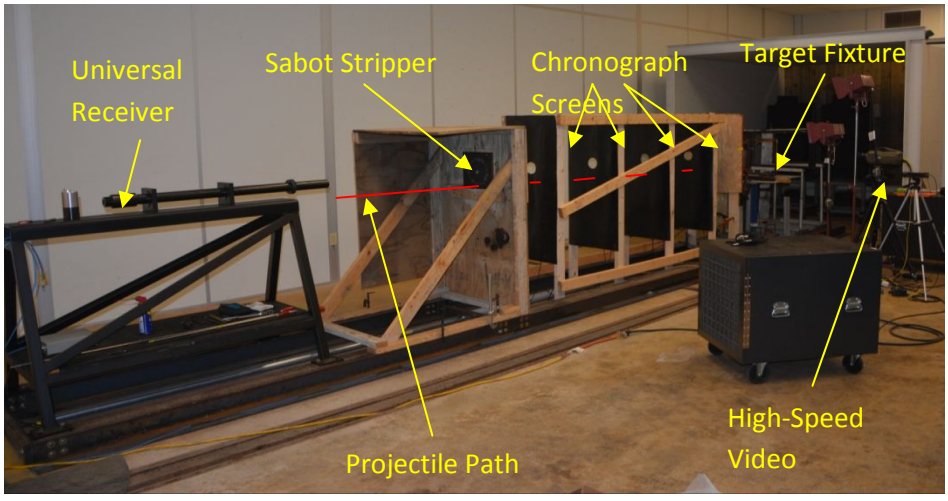

Figure 2. Ballistic Research Facility.

For the purposes of this study, the calculation of V_{50} was determined by the arithmetical mean of four shots (the two lowest velocity complete perforations, and the two highest velocity partial penetrations) that all were within a 150ft/s (46m/s) band within the zone of mixed results, in accordance with MIL-STD-662F.[6]

Sufficiently small projectiles were desirable in order to maintain high impact velocities, reduce the overall target thickness, and reduce the overall cost of the study. Stainless steel 2.1 grain spheres measuring 0.13 inches in diameter were readily available and were found to produce repeatable penetrations into the polymer panels.

Figure 3. 0.50 Caliber Cartridge with Sabot and Projectile.

As shown in Figure 3, the spheres were loaded into four-petal 0.50 caliber, smooth sabots, machined from acetal homopolymer. Sabots were then seated in 0.50 caliber cartridges with a specific powder load. The volume of powder loaded into each cartridge was adjusted to provide the desired velocity (in accordance with calibrated powder measurements), and the remaining space in the projectile was filled with an organic material (ground walnut shells).

The polymers used in this investigation were all purchased from a warehouse supplier that provided material property data sheets for all products. The material property sheets were used to compile basic material properties, shown in Table 2.

While some manufacturers listed a plethora of material property data, others listed only a handful of values, which limited the points of comparison between the samples. Therefore, only material properties that were available for all materials were used in this investigation.

1. Theory

3.1 DMA Analysis

A typical DMA plot of *E'*, *E''*, and *tan δ* measured at two frequencies versus temperature is shown in Figure 4. All three of these properties remained relatively constant at the lower end of the temperature range studied. At higher temperatures, depending on the particular material, the polymers experienced thermal transitions resulting in drastic decreases in *E'*. The transition can be attributed to either a glass transition or a crystalline melt according to the polymer morphology. In some cases, semicrystalline

polymers are known to undergo secondary thermal transitions such as a glass transition at temperatures far below the lower temperature limit experienced in this study, e.g., Delrin is known to display a glass transition, T_g, at -60 °C.

Table 2. Polymer Material Properties.

Material	Specific Gravity (g/cc)	Tensile Strength, Yield (psi)	Elgonation at Break (%)	Tensile Modulus (ksi)	Flexural Modulus (ksi)	Compressive Strength (psi)	Deflection Temperature at 264 psi (F)
HDPE [9]	0.96	4100	600.0	116	185	2900	140
Polycarbonate [10]	1.2	9000	110.0	340	345	12500	270
Acetal Resin [11]	1.42	11000	25.0	450	420	5200	257
Temp. Stabilized UHMW Polyethylene [12]	0.94	6800	300.0	72.5	80	3000	116
Moisture Resistant UHMW Polyethylene [13]	0.93	5800	300.0	80	87	3000	116
Nylon 6/6 [14]	1.14	12000	25.0	350	440	5000	194
Nylon (6/12) [14]	1.06	8000	20.0	300	275	2400	142
Cast Acrylic [15]	1.19	10800	4.0	450	421	17500	185
ABS [16]	1.03	6,000	40.0	330	300	9400	197
PET [17]	1.38	12500	20.0	470	430	19500	175
PEEK [18]	1.31	14100	20.0	630	594	20000	320

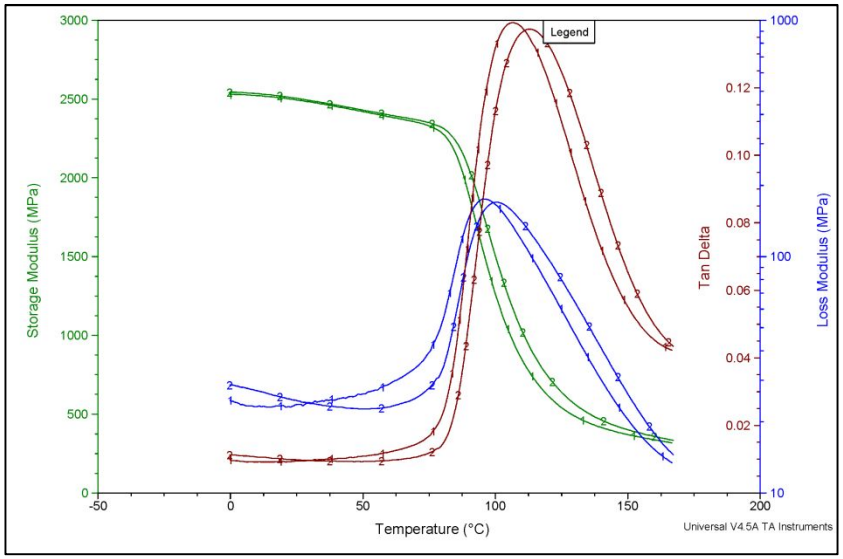

Figure 4. DMA Plot of Polyester.

All materials tested were viscoelastic solids at room temperature, i.e., the amorphous polymers were below T_g, and the crystalline polymers were below their melting temperature, T_m, at room temperature.

It is worth noting that the heat of deformation due to high-velocity impact is not insignificant, especially in regards to polymer armor materials. As seen in Figure 4. DMA Plot of Polyester., even a 50 °C rise in temperature would be sufficient to elevate some polymers into the transition region, where their responses becomes much less like an elastic solid and much more like a viscous fluid. Because these impact studies were highly localized, the volume of material affected by the heat of deformation was small, thus the heat per-unit volume was quite large and sufficient to cause thermal transitions in the vicinity of the penetration event. While these characteristics of polymer ballistics are worth mentioning and almost certainly have an effect on the overall performance of the samples, the authors theorized that due to the high strain-rates ($>10^4$) associated with these impact events, the effects from deformation are either captured in other material properties or would not dominate the overall performance of the materials, and are thus beyond the scope of this paper.

Many properties of polymers are known to be strongly rate dependent in addition to the temperature dependence already discussed. Because high-rate testing is often difficult to perform in a controlled fashion with isolated variables, the principle of time-temperature superposition is useful to approximate polymer response at high rates. The premise of time-temperature superposition is that a similar response can be measured at low rate and low temperature as is observed at high rate and high temperature. Therefore, a relatively low strain-rate mechanical test can be performed at very low temperature and the results extrapolated to represent an ambient temperature event at high strain-rate. Though beyond the scope of the present study, the time-temperature superposition approach may further elucidate the connections among studied properties and ballistic response.[4]

3.2 Statistical Analysis

There are many practical guidelines to fitting a statistical model to experimental data. Ideally, the ratio of observations (n) to model parameters (p) should exceed 10.[7] However, testing hundreds of polymer types is cost prohibitive to this investigation, and the overall goal was not necessarily to define a firm model that predicts V_{50} for all polymeric materials, but rather to determine what properties govern high-speed penetration events in these materials and are thus statistically valuable.

A major statistical issue when attempting to model experimental phenomena with relatively few observations is the issue of over-fitting and bias.

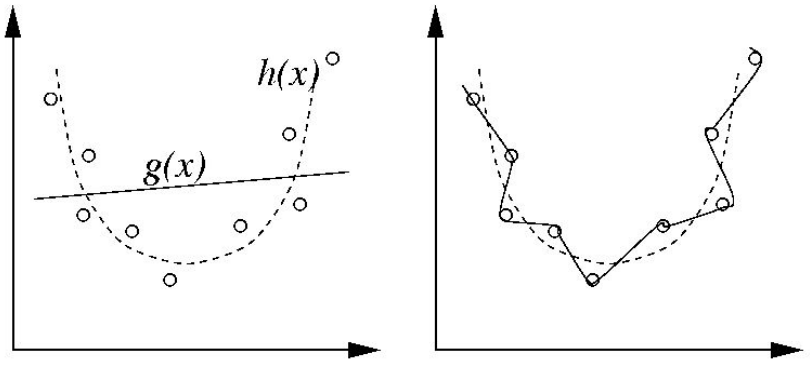

Figure 5. Bias vs. Over-fitting. [8]

Figure 5 shows two examples of the same parabolic data set with the ideal statistical model represented by the dashed line, and the model represented by the solid line. The model on the left shows a two-variable model that has the virtue of being simple; however, it does not show good fit and would not be accurate for predictions. This is an example of a high-bias model. Conversely, the model on the right fits the data exactly and is zero bias, yet it would still be incapable of accurately predicting new measurements. This model is an over-fit to the data. The challenge to statisticians is to determine the best fit model, with an appropriate level of bias, without over-fitting. [8]

Perhaps the most well known test for model utility is the multiple coefficient of determination, R^2, that effectively relates the variation of the response variable (V_{50} in this case) that is attributable to the model parameters. While R^2 is a valid test of model fit, it does not address the issue of model over-fitting. A simple method to avoid this is to simply conduct a best subsets analysis, and then observe as standard deviation (S) converges to a near constant number. The model with the least number of variables at the converged standard deviation will be the best fit. Finally a third criterion available to select a best fit model is the C_p criterion, which is based on the total mean square error of the regression model. Simply put, the best model fit contains a value of C_p near p + 1, where p is the number of variables or parameters in the model. All three methods will be employed to select the best regression model for the given experimental results.

Once a model is selected, validity will be determined through a process known as cross-validation. In this process, one of the observations will be omitted from the data set during model fitting, so that it has no influence on the model itself. The new model will then be run on the omitted data to determine how accurately the model predicts the observation as compared to the original model with all data included. This process is automated in Minitab, and the cross-validation results in an adjusted (reduced) R^2 value that will be a more realistic indicator of how well the model will accurately predict future experiments. As long as the $R^2_{(pred)}$ is sufficiently close to the original value, then the model will be deemed statistically useful.[7]

Table 3. Normalized Results of Ballistic and DMA Analyses at 21°C.

Material	V_{50}	Storage Modulus	Loss Modulus	Tan δ	Driving Stress
HDPE	0.5454	0.7909	0.2584	0.1976	0.7768
Polycarbonate	0.7527	0.1294	0.2139	1.0000	0.2113
Acetal Resin	0.8636	1.0000	0.2308	0.1409	1.0000
Temp. Stabilized UHMW Polyethylene	0.5347	0.2905	0.1198	0.2494	0.3116
Moisture Resistant UHMW Polyethylene	0.5347	0.2876	0.1154	0.2428	0.3008
Nylon 6/6	0.8147	0.7804	0.1284	0.0996	0.7946
Nylon (6/12)	0.7238	0.6611	0.0930	0.0851	0.6670
Cast Acrylic	1.0000	0.9653	1.0000	0.6268	0.9461
ABS	0.6856	0.5807	0.1131	0.1178	0.5785
PET	0.8422	0.7760	0.1035	0.0807	0.7823
PEEK	0.9735	0.9222	0.1245	0.0817	0.5590

2. Results

As stated above, the DMA process tabulates storage and loss moduli and tan δ over a range of temperatures and frequencies. Due to limitations of the test apparatus, not all samples could be tested at the highest frequency of 100Hz, thus the data from highest rate that was available for all materials (10Hz) were used for the statistical analysis. Likewise, because the panels were ballistically tested at room temperature 21.0°C, only DMA data at that temperature were considered. Data were normalized by dividing all values by the maximum observed value for each variable. The full table of normalized V_{50} results and DMA data at 21.0°C and 10Hz is provided below.

Data in Table 2 were then normalized in the same fashion as the experimental data, and the two tables were combined for statistical analysis in Minitab. The best-subsets analysis quickly eliminated first-order predictors that had little statistical value on the prediction of V_{50}, and a clear positive trend was found between four predictors, i.e., Loss Modulus (E''), tensile modulus (E), tensile yield strength (σ_Y) and elongation to break (ε_{break}). The results of the final Minitab best subsets analysis are shown in Figure 6, and the regression model that was ultimately selected is highlighted in yellow.

Response is V50

			Mallows		Parameters							
Vars	R-Sq	R-Sq(adj)	Cp	S	A	B	C	D	E	F	G	H
1	89.2	88.0	92.9	0.057737				X				
1	86.8	85.4	114.8	0.063752					X			
1	77.5	75.0	201.0	0.083315	X							
2	97.0	96.2	22.9	0.032390				X				X
2	95.5	94.3	36.8	0.039599					X			X
2	90.5	88.1	83.2	0.057542	X			X				
3	99.1	98.7	5.4	0.019006	X			X				X
3	98.3	97.6	12.6	0.025889			X		X			X
3	97.7	96.7	18.2	0.030133			X	X				X
4	99.4	99.0	4.4	0.016389	X	X	X					X
4	99.2	98.6	6.7	0.019628	X	X			X			X
4	99.1	98.6	7.0	0.019958	X			X	X			X
	.	.	.	.								
	.	.	.	.								
	.	.	.	.								
8	99.8	98.9	9.0	0.017332	X	X	X	X	X	X	X	X

Figure 6. Minitab Best Subsets Analysis.

Parameters that correspond to A-H in Figure 6 are Specific Gravity (A), Tensile Yield Strength (B) Elongation to Break (C), Tensile Modulus (D), Flexural Modulus (E), Deflection Temperature at 264psi (F), Storage Modulus (G), and Loss Modulus (H).

The yellow highlighted model was selected due to the three basic criterion described in the previous section, i.e., 1) a sufficiently high R^2 of 99.4% suggests excellent correlation between the model and the measured V_{50} values, 2) the standard deviation (S) does not change appreciably by adding more variables, and 3) a C_p near p+1 = 5 indicates a low level of bias in the model. Note that the grey highlighted model in Figure **6** is also a good fit albeit slightly more biased. This model shows that the effect of neglecting elongation to break has a minor impact on the overall predictive capability of the model.

The linear regression model takes the form of Equation 2.

$$V_{50} = \beta_0 + \beta_1\sigma_Y + \beta_2\varepsilon_{break} + \beta_3 E + \beta_4 E'' \quad (2)$$

where: $\beta_0 = 0.415$
$\beta_1 = 0.202$
$\beta_2 = -0.0491$
$\beta_3 = 0.336$
$\beta_4 = 0.193$

Finally, the cross-validation analysis reveals a predicted R^2 value of 93.7%, indicating that the model parameters are indeed valid and useful. The final regression Minitab printout is provided as Appendix A; results of the cross-validation analysis are highlighted.

Table 4. Model Results and Error.

Material	V_{50} (Experimental)	V_{50} (Model)	Error (%)
HDPE	0.5454	0.5360	-1.7
Polycarbonate	0.7527	0.7571	0.6
Acetal Resin	0.8636	0.8546	-1.0
Temp. Stabilized UHMW Polyethylene	0.5347	0.5493	2.7
Moisture Resistant UHMW Polyethylene	0.5347	0.5381	0.6
Nylon 6/6	0.8147	0.7959	-2.3
Nylon (6/12)	0.7238	0.7054	-2.5
Cast Acrylic	1.0000	1.0022	0.2
ABS	0.6856	0.6950	1.4
PET	0.8422	0.8625	2.4
PEEK	0.9735	0.9748	0.1

3. Discussion and Conclusions

The small degree of correlation between tan δ and ballistic limit was surprising. Because loss modulus and storage modulus are both functions of tan δ, the assumption was made that all three variables would show similar levels of correlation. Instead, the relatively high correlation of loss modulus to the ballistic limit suggests that even though all DMA values are related, the degree to which each polymer is capable of dissipating energy (defined by loss modulus) has more bearing on the overall performance against high-velocity, low-mass projectiles.

The significance of the regression model is not necessarily as predictor of ballistic resistance in other materials, but rather as an indicator of the physical material properties that dominate high velocity penetrations into polymer materials. Because all data were normalized prior to the statistical analysis, the coefficients of the model, β_1 through β_4, act as statistical weight functions for each of the four variables in the model. This shows that tensile modulus is the dominant material property governing high-speed polymer penetrations, while tensile strength and loss modulus have roughly the same level of influence,

and elongation has a negative correlation to ballistic resistance and the least impact overall, as expected based on comparison of the highlighted models in the best subsets analysis (Figure **6**).

The values of tensile modulus, tensile strength, and elongation taken from the product data sheets provided by the supplier were measured under quasistatic strain conditions and at ambient temperature. Of interest would be analysis of these same parameters measured at very low temperature. This approach has proven valid in other ballistic applications of thermoplastics.[19] The time-temperature superposition principle could then be applied to approximate material properties at high strain-rate at 21 °C. The correlation of tensile modulus, tensile strength, and elongation with V50 could thus be assessed for higher strain-rates such as those experienced in ballistic penetration events.

4. Acknowledgements

The authors wish to acknowledge the contributions of Predictive Design Technologies and the Mississippi State University Center for Advanced Vehicular Systems (CAVS) for their contributions to the DMA analyses included in this study.

Funding and permission to publish were granted by Director, Geotechnical and Structures Laboratory.

5. References

[1] Roland, C.M. et al. *Factors influencing the ballistic impact resistance of elastomer-coated metal substrates.* Philosophical Magazine. 2013.
[2] Harpell, G.A. et al. US Patent 4,748,064, Ballistic Resistant Composites.
[3] ASTM-D4065-12, Standard Practice for Plastics: Dynamic Mechanical Properties: Determination and Report of Procedures. 2012.
[4] Menczel, J.D; Prime, R.B. Thermal Analysis of Polymers, Fundamentals and Applications. 2009.
[5] Jordan, J.B.; Naito, C.J. *An Experimental Investigation of the Effect of Nose Shape on Fragments Penetrating GFRP.* International Journal of Impact Engineering. 2012.
[6] MIL-STD-662F, Department of Defense Test Method Standard, V50 Ballistic Test for Armor. 1997.
[7] Mendenhall, W.; Sincich, T. Regression Analysis, A Second Course in Statistics, 7th Ed, 2012.
[8] http://www.willamette.edu/~gorr/classes/cs449/overfitting.html
[9] King Plastic Corporation, King KPC ® HDPE Data Sheet, KPC_HDPE_02/2011-5M. 2011.
[10] Bayer Material Science, Makrolon® WG Sheet, MAKWG 0412. 2012.
[11] Ensinger Inc., Delrin ® Acetal Homopolymer, http://www.ensinger-inc.com/products.cfm?page=product&product=delrinandreg;+acetal+homopolymer, 2014.
[12] Quadrant EPP USA, Inc., Quadrant EPP TIVAR ® H.O.T. UHMW-PE Premium Heat Stabilized/Anti-Oxidant Filled (ASTM Product Data Sheet). 2013.
[13] Quadrant EPP USA, Inc., Quadrant EPP TIVAR ® 1000 UHMW-PE, Virgin (ASTM Product Data Sheet). 2013.
[14] Ensinger Inc., Tecamid 612 – Extruded Nylon 612. http://www.ensinger-inc.com/products.cfm?page=product&product=tecamid+612+-+extruded+nylon+612. 2014.
[15] Reynolds Polymer Technology Inc., R-Cast ® Sheet Product Data Sheet. 2012.
[16] King Plastic Corporation, King KPC ® ABS Data Sheet, KPC_ABS_02/2011-5M. 2011.

[17] Ensinger Inc., Tecapet ®, http://www.ensinger-inc.com/products.cfm?page=product&product=tecapet
[18] Advanced Polymer Technologies, Semilon PK (PEEK). 2012.
[19] Maljkovic and Rushing, US Patent 8,240,252, Ammunition Casing. 2013.

Appendix A: Minitab Final Regression

Regression Analysis: V50 versus Tensile Strength, Elgonation at Br, ...

```
The regression equation is
V50 = 0.415 + 0.202 Tensile Strength, Yield - 0.0491 Elgonation at Break
      + 0.336 Tensile Modulus + 0.193 Loss Modulus


Predictor                   Coef  SE Coef      T      P
Constant                 0.41461  0.02690  15.41  0.000
Tensile Strength, Yield  0.20211  0.04809   4.20  0.006
Elgonation at Break     -0.04914  0.02660  -1.85  0.114
Tensile Modulus          0.33560  0.04210   7.97  0.000
Loss Modulus             0.19343  0.02033   9.52  0.000


S = 0.0163886   R-Sq = 99.4%   R-Sq(adj) = 99.0%

PRESS = 0.0167238   R-Sq(pred) = 93.97%


Analysis of Variance

Source          DF        SS        MS       F      P
Regression       4  0.275837  0.068959  256.75  0.000
Residual Error   6  0.001612  0.000269
Total           10  0.277448


Source                   DF    Seq SS
Tensile Strength, Yield   1  0.214976
Elgonation at Break       1  0.009259
Tensile Modulus           1  0.027283
Loss Modulus              1  0.024319


      Tensile
     Strength,
Obs      Yield      V50      Fit   SE Fit  Residual  St Resid
  1       0.29  0.54544  0.53601  0.01521   0.00943      1.54
  2       0.64  0.75269  0.75709  0.00514  -0.00440     -0.28
  3       0.78  0.86359  0.85460  0.00617   0.00899      0.59
  4       0.48  0.53467  0.54929  0.01062  -0.01463     -1.17
  5       0.41  0.53467  0.53812  0.00906  -0.00345     -0.25
  6       0.85  0.81466  0.79586  0.01004   0.01880      1.45
  7       0.57  0.72379  0.70543  0.00885   0.01835      1.33
  8       0.77  1.00000  1.00223  0.01618  -0.00223     -0.87
  9       0.43  0.68562  0.69500  0.01355  -0.00938     -1.02
 10       0.89  0.84224  0.86253  0.00814  -0.02029     -1.43
 11       1.00  0.97355  0.97476  0.01269  -0.00121     -0.12

No evidence of lack of fit (P >= 0.1).
```